CHAPTER 5

Visco-elastic measurements in the nematic phase of a few hockey stick-shaped liquid crystals

5.1. Introduction

Bent-core nematics (BCNs) have attracted considerable interest because of a number of unusual features and exceptional properties demonstrated by this class of liquid crystalline phases. The nematic (*N*) phases of bent-core compounds have been characterized by several remarkable properties like great flexoelectric response [1, 2], extraordinary electro-convection patterns [3–5], low frequency dielectric relaxation [6], magnetic field induced isotropic to nematic phase transition [7], biaxiality [8–11] and ferro-nematic phase [12], some of which again may be related to the presence of smectic-like clusters in this phase. Bent-core nematic phases are regarded as potential candidates for electro-optic applications.

From the view point of practical applications of liquid crystals, rotational viscosity (γ_1) serves as a very important material parameter, deciding device performance through the switching behavior of the concerned material in external fields. The rotational viscosity, which is related to the torque associated with the rotation of liquid crystal (LC) directors during molecular reorientations and thereby describes the force of internal friction among LC directors, depends on the structural form and constitution of the LC molecules, intermolecular interactions and sample temperature. For calamitic LCs

although the typical magnitude and temperature dependence of molecular relaxation time (τ_0) and hence, rotational viscosity are reasonably well ascertained [13–15], reports related to the study of rotational viscosity in bent-core or hockey stick-shaped molecules exhibiting a nematic phase are still scarce [16–19]. For bent-core LCs, the angular design of the molecules and hence, the steric hindrance and molecular association have a crucial influence on the visco-elastic behavior. Recent investigations on some bent-core nematics do reveal rotational and flow viscosities respectively of about one order and two orders of magnitude higher than calamitic nematics [16, 17]. Furthermore, there is also evidence of BCN demonstrating a slightly higher value of γ_1 compared to usual rod-like LCs [18]. Again the hockey stick-shaped molecules possess a shape intermediate between the classical rod-like molecules and the conventional bent-core molecules and therefore are expected to exhibit γ_1 values relatively lower than the symmetric bent-shaped molecules. Hence, it is interesting to study the visco-elastic properties in the nematic phase of hockey stick-shaped compounds.

In the preceding chapter (i.e., chapter 4) the study on structural and mesomorphic properties of five members of a homologous series of laterally methyl substituted hockey stick-shaped compound 4-(3-*n*-alkyloxy-2-methyl-phenyliminomethyl)phenyl 4-*n*-alkyloxycinnamates from polarizing optical microscopy, X-ray diffraction, NMR, optical birefringence, dielectric and electro-optical techniques have been reported. Interestingly, in these compounds the lateral substitution by a methyl group in the obtuse angle between the *m*-alkyloxy-chain attached to the terminal phenyl ring and the azomethine connecting group leads to the suppression of the smectic *A* phase along with the emergence of the nematic phase in a certain temperature range. Such occurrence of nematic phases is quite remarkable among the mesophases of bent LCs and their presence certainly enhances their potential for application. In continuation of the previous work, in this chapter the results on the measurements of rotational viscosity in the nematic phase of four members

of the above mentioned hockey stick-shaped compounds have been presented [20]. In order to determine the rotational viscosity as a function of temperature, knowledge of the splay elastic constant and also the relaxation time is required. Similar to the previous study on the 4-cyanoresorcinol bent-core compounds, the measurements of relaxation time have been performed by two different probing methods *viz.* capacitive decay and optical phase-decay-time measurement methods. Necessary splay elastic constant was determined from a study of the electric field induced Freedericksz transition and from the dielectric anisotropy of the molecules. Moreover, for the determination of the relaxation time by optical method, the optical phase retardation of the sample filled cell is required which was obtained from optical birefringence measurements as described in chapter 4. The birefringence values were also compared with those determined from thin prism technique. In addition, the temperature dependence of bend elastic constant has also been determined to observe the nature of the temperature dependence of elastic anisotropy. From an analysis of the dielectric permittivity data in the isotropic phase, close to the nematic–isotropic (*N–I*) phase transition, the pretransitional behavior has also been explored. Thus, in this work the temperature dependence of birefringence, dielectric anisotropy, splay and bend elastic constants, relaxation time and hence the rotational viscosity of the hockey stick-shaped compounds have been determined. The results have been compared with the conventional rod-like nematics and also those for traditional symmetric bent-core nematogens and explained by considering the exotic structural geometry of the hockey stick-shaped molecules and the related unusual inter-molecular interactions appearing within the mesophase.

5.2. Refractive index measurements

The temperature dependant variation of the birefringence ($\Delta n = n_e - n_o$) at a wavelength of λ = 632.8 nm as obtained from the thin prism method for the compounds is shown in figures 5.1(a)–(e). Birefringence obtained from the

optical transmission (O.T.) measurements as presented in the previous chapter, has also been included for comparison. The agreement between the two sets of values obtained from these two different approaches is fairly good in the limited temperature range. However for all compounds, well within the nematic phase, the values of Δn obtained from the transmission method are found to be slightly higher than those measured by the thin prism technique. Such a trivial disparity for these two measuring procedures has been interpreted in terms of the greater sample thickness (~20–40 times) and the resulting decrease in the surface anchoring due to which the molecular ordering is retained somewhat less than in thin cells of much smaller dimensions [21].

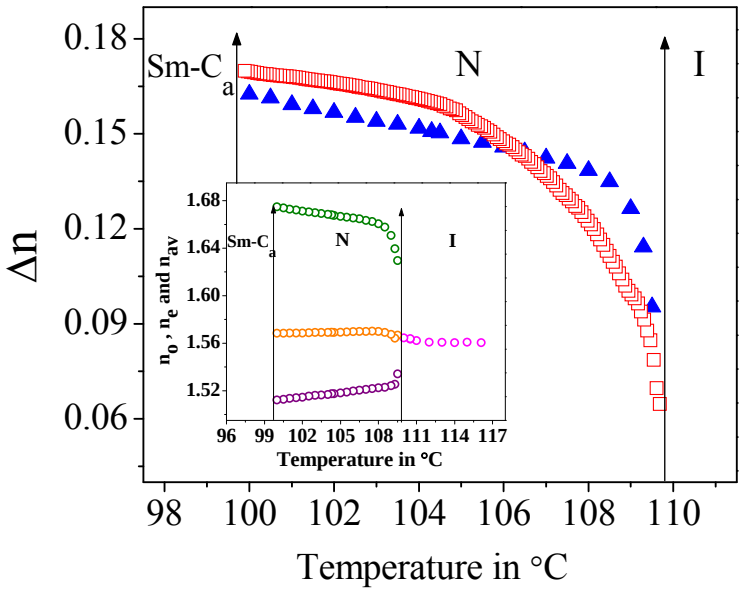

(a)

Figure 5.1. Experimental values of refractive indices n_o and n_e and birefringence ($\Delta n = n_e - n_o$) as a function of temperature for (a) compound **1**. ○ : n_o; ○ : n_e; ○ : n_{iso}; ○ : n_{av}; ▲ : birefringence (from thin prism method); □ : birefringence (from optical transmission measurement).

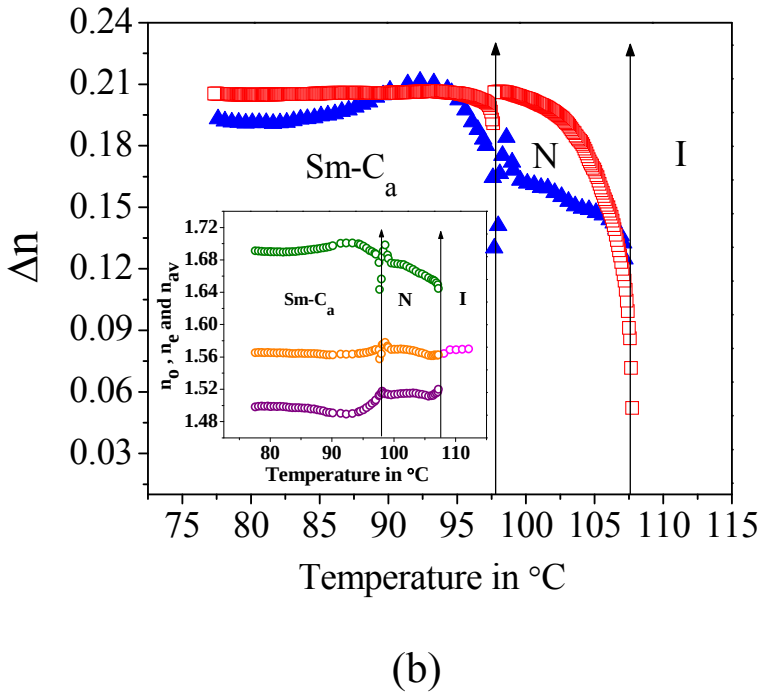

(b)

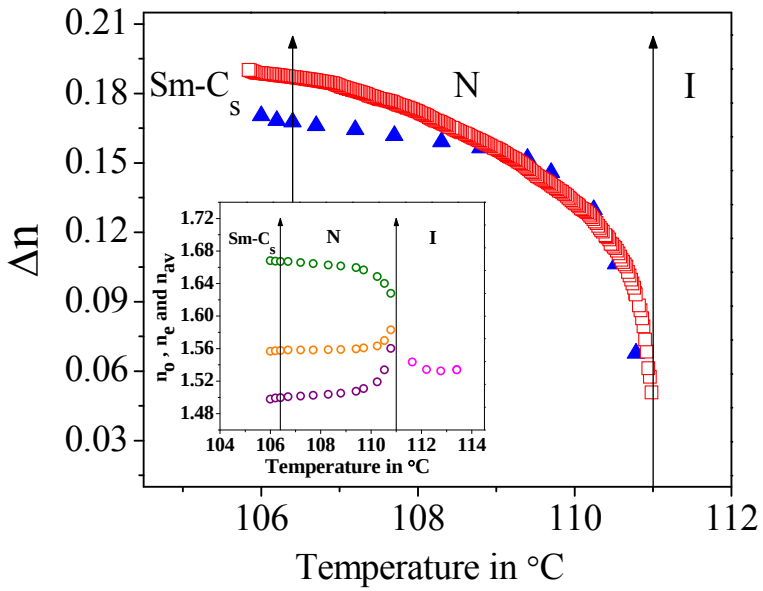

(c)

Figure 5.1. (cont'd). Experimental values of refractive indices n_o and n_e and birefringence ($\Delta n = n_e - n_o$) as a function of temperature for (b) compound **2**; (c) compound **3**. ○ : n_o; ○ : n_e; ○ : n_{iso}; ○ : n_{av}; ▲ : birefringence (from thin prism method); □ : birefringence (from optical transmission measurement).

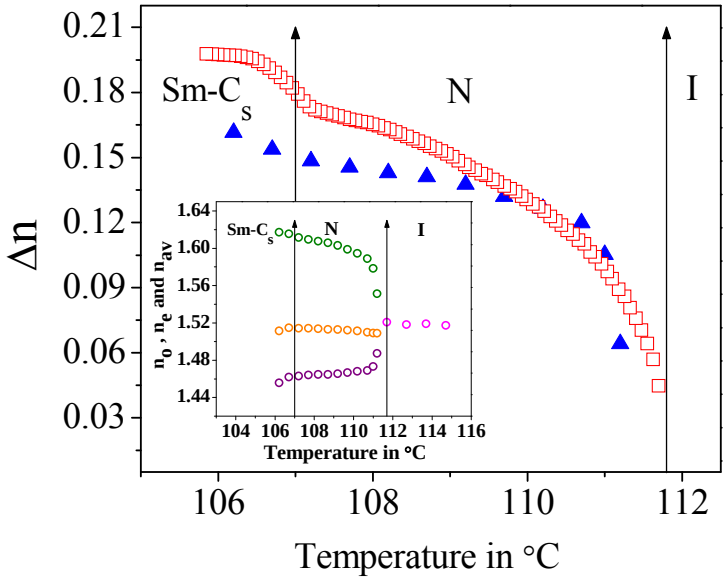

(d)

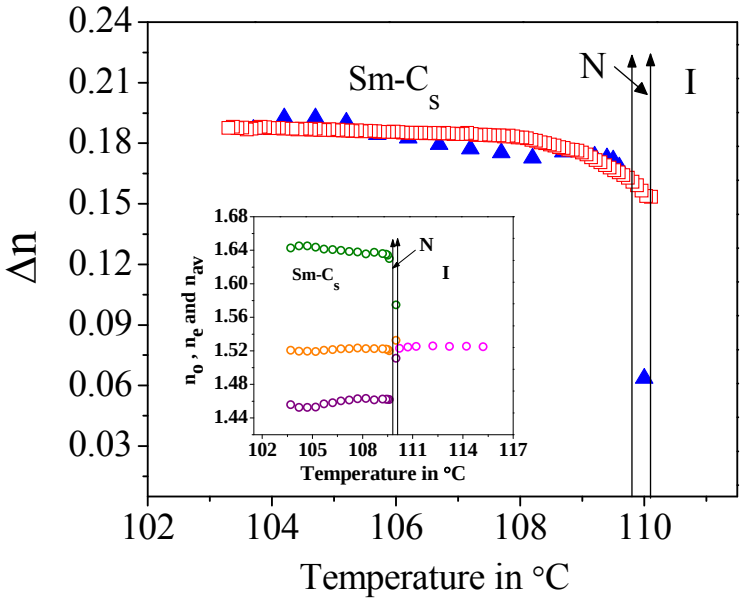

(e)

Figure 5.1. (cont'd). Experimental values of refractive indices n_o and n_e and birefringence ($\Delta n = n_e - n_o$) as a function of temperature for (d) compound **4**; (e) compound **5**. ○ : n_o; ○ : n_e; ○ : n_{iso}; ○ : n_{av}; ▲ : birefringence (from thin prism method); □ : birefringence (from optical transmission measurement).

The temperature dependence of the principal refractive indices n_o and n_e, the average refractive index (n_{av}) as well as the refractive index in the isotropic phase (n_{iso}) are also shown in the insets of figures 5.1(a)–(e). Both, n_o and n_e slightly vary within the nematic phase. For most of the compounds the isotropic refractive index n_{iso} is found to have more or less the same value as the average component n_{av} of the refractive index in the *N* phase while for compounds **1** and **3**, n_{iso} is slightly lower than n_{av}. This result is in agreement with the finding of others for distinct oxazole based bent-core nematogens revealing no divergence of the nematic mean refractive index from the isotropic value (n_{iso}) [22]. Moreover, for calamitic LCs it is rather usual to have a slightly higher value of n_{av} than n_{iso}.

On cooling from the isotropic phase, a sharp enhancement in the birefringence (Δn) is observed at the nematic–isotropic transition, essentially due to the increase in the nematic order *via* a significant growth of the cybotactic clusters from the disordered fluid state and their alignment by strong surface anchoring which in turn is facilitated in the rapid growth of the optical anisotropy of the media. For these compounds such kind of short range ordering has also been revealed by small angle X-ray diffraction measurements (discussed in chapter 4). On further cooling, well within the mesophase the increase in Δn is relatively small. Fortunately, for compound **2**, it was possible to measure both the ordinary and the extraordinary components of the refractive indices in the anticlinic smectic *C* phase, even though it is well known that the measurement of Δn is considerably difficult in the higher ordered smectic phases due to the poor alignment compared with that in the *N* phase and sometimes also due to strong absorption in the medium. It has been observed that the birefringence values remain more or less constant in that region. In the case of compound **5** it was possible to determine the n_o and n_e values in both the *N* and Sm-C_s phases. Within the Sm-C_s phase both refractive indices (n_o, n_e) and hence the birefringence remain more or less constant throughout the mesophase. It is also observed that in general the change in

birefringence is continuous across the Sm-C_s–N transition indicating a very weak first order or a second order nature of that transition while the discontinuity in the Δn curve at the Sm-C_a–N transition (compound **2**) clearly implies the first order nature of that transition.

5.3. Static dielectric permittivity measurements

The temperature dependences of the dielectric parameters [$\varepsilon_{\parallel}$, $\varepsilon_{\perp}$, ε_{iso} and $\varepsilon_{av} = \{1/3(2\varepsilon_{\perp}+\varepsilon_{\parallel})\}$] for two representative compounds **2** and **4** are illustrated in figures 5.2(a)–(b) while variation of the dielectric anisotropy ($\Delta\varepsilon = \varepsilon_{\parallel} - \varepsilon_{\perp}$) for all the mesogens are shown in figure 5.3. In compounds **2** and **4** it is observed that on cooling from the isotropic state, $\Delta\varepsilon$ [inset of figures 5.2(a)–(b)] primarily grows with decreasing temperature in the N phase and then remains more or less constant or slightly diminishes after attaining a maximum and further continues to decrease sharply throughout the entire Sm-C_s phase. Hence, within the N and Sm-C_s phases the anisotropy ($\Delta\varepsilon$) always assumes small positive values. Interestingly, a pronounced drop is observed in the $\varepsilon_{\parallel}$ values at the transition from the nematic to the smectic C_a phase (compound **2**) while the drop is somewhat smaller at the smectic C_s to smectic C_a phase transition (compound **4**). However, in both the cases, it leads to a cross over in the two dielectric components ($\varepsilon_{\parallel} < \varepsilon_{\perp}$) just on entering the low temperature anticlinic phase, i.e., causing the $\Delta\varepsilon$ values to be negative in the Sm-C_a phase. On further cooling, the two permittivity components ($\varepsilon_{\parallel}$, $\varepsilon_{\perp}$) retain their trends but the enhancement in $\varepsilon_{\perp}$ or the decrease in $\varepsilon_{\parallel}$ is now quite gradual. Hence, a temperature dependent sign reversal in the dielectric anisotropy is observed within the anticlinic smectic C phase for all the hockey stick-shaped compounds under study. Similar sign inversion in $\Delta\varepsilon$ has formerly been observed in the Sm-C_a phase for a related three ring hockey stick-shaped compound [23] and has also been reported by others for symmetric bent-shaped nematogens [24] and for some calamitic molecules as well [25]. This anomaly may be explained by considering a drastic re-orientation of the molecules at the

phase transition: the molecular long axes are oriented parallel to the aligning surface in the Sm-C_s phase of the surface aligned bulk sample and the layers are tilted with respect to the surface. However, the anticlinic arrangement of the molecules in the Sm-C_a phase forces the layers to align parallel to the surface and the molecular long axes to be tilted with respect to it. Such a tilted molecular arrangement in the Sm-C_a phase certainly causes a significant drop in the parallel component of the molecular dipole moment ($\mu_{\|}$), i.e., along the molecular long axis and thereby reduces the longitudinal component of dielectric permittivity ($\varepsilon_{\|}$) to a considerable extent. Additionally, the dipole–dipole interactions between molecules of the same smectic layer are stronger than those between molecules of adjacent layers. This causes an enhancement in the antiparallel dipolar correlation along the molecular director which lowers the $\varepsilon_{\|}$ values, too. For calamitic molecules the details of the analysis regarding such interactions and their influence on the molecular parameters have already been reported by de Jeu *et al.* [25]. Moreover, from previous NMR conformational studies [26] for a group of closely related hockey stick-shaped compounds, it has also been found that the hockey stick-shaped molecule behaves more or less like a calamitic (rod-like) molecule in orthogonal and synclinically tilted smectic phases, resulting in the normal temperature variation of the dielectric parameters. However, at the transition to the smectic C_a phase due to the reorientation in the molecular part containing the 3-alkyloxyphenyl fragment a more hockey stick like shape is attained and the effect of the structural bent on the mesogenic behavior becomes more pronounced. Such conformational change of molecular fragment may also be associated with the present system as well, although the entire scenario may be more complex and an exact knowledge requires a precise conformational analysis as have been done based on NMR measurements in Ref. [26]. Recently, an inversion in dielectric anisotropy has also been observed for an achiral bent-shaped nematogen at the Sm-*C*–*N* transition by Sathyanarayana *et al.* [24]. They have argued that along with the effect of enhanced antiparallel

dipolar correlation along the molecular long axis, the formation of smectic layering and the rotational hindrance emerging from the local layer packing of the bent molecules also have a crucial influence both on the reduction of the $\Delta\varepsilon$ values as well as affecting the rate of variation of the same with temperature. The present study seems to fit well with the above model in which the plausible conformational alteration of the hockey stick-shaped compounds indeed causes the molecules to behave more like a bent shaped structure rather than the simple straight-core geometry and leads to a considerable diminution in $\Delta\varepsilon$ for the reasons discussed above.

For compounds **1** and **2**, a significant pretransitional effect is observed in the vicinity of the Sm-C_a–N phase transition, may be due to the strong growth of the cybotactic clusters and the enhancement in their dimension which again stimulates the smectic like behavior prior to that transition.

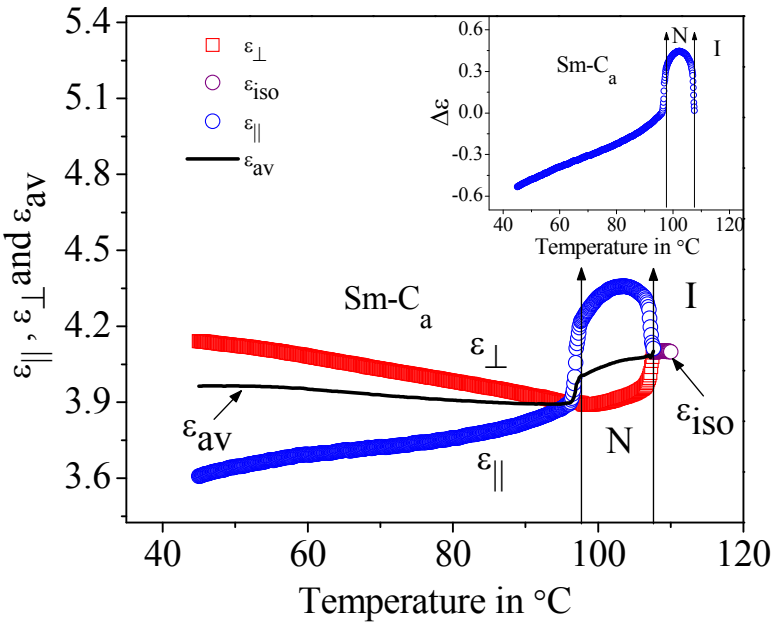

(a)

Figure 5.2. Temperature variation of dielectric parameters [$\varepsilon_{\parallel}$, $\varepsilon_{\perp}$, ε_{av}, ε_{iso} and $\Delta\varepsilon$ (inset)] for (a) compound **2**.

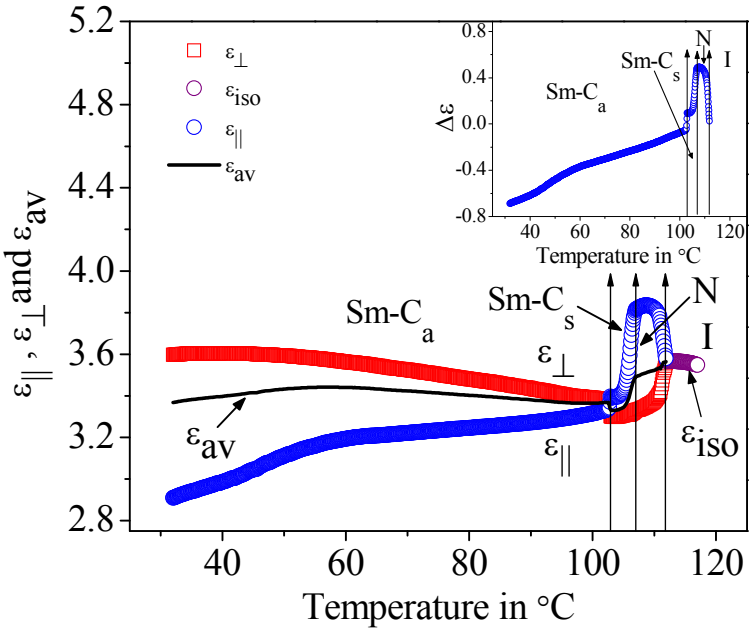

(b)

Figure 5.2. (cont'd). Temperature variation of dielectric parameters [$\varepsilon_{\parallel}$, $\varepsilon_{\perp}$, ε_{av}, ε_{iso} and $\Delta\varepsilon$ (inset)] for (b) compound **4**.

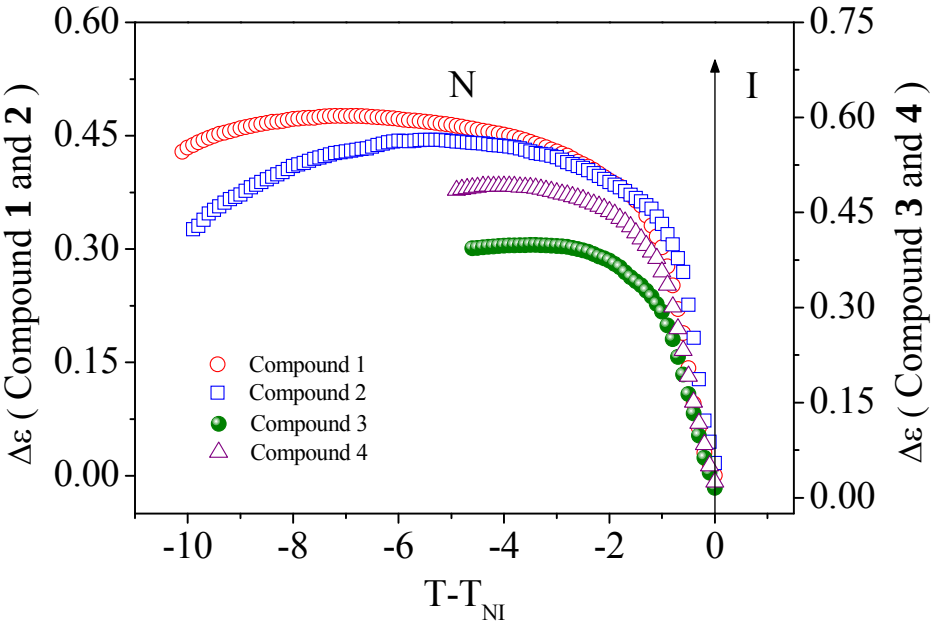

Figure 5.3. Temperature dependence of the dielectric anisotropy ($\Delta\varepsilon$) in the nematic phase for the compounds **1**–**4**.

Moreover, due to the contribution from the orientational polarization and density, although it is anticipated that the average component of the dielectric permittivity (ε_{av}) will increase with the lowering of temperature [27], in the present case for all the compounds it was found that the value of the isotropic dielectric permittivity (ε_{iso}) extrapolated in the mesophase is always greater than the average component of the dielectric permittivity (ε_{av}). Such a behavior is perhaps due to the antiparallel correlation between the neighboring molecular dipoles in the mesogenic medium [28].

Furthermore, recently, a number of attempts have been made to investigate the pretransitional effects at the *N–I* phase transitions in calamitic molecules [29–33]. However, for hockey stick-shaped molecules, no such report has been made so far. Hence, it is also of much interest to study the pretransitional behavior at the *N–I* phase transitions in the hockey stick-shaped compounds under investigation. For this purpose, the temperature dependence of the static dielectric permittivity in the isotropic phase can suitably be employed for obtaining a reliable description of the pretransitional behavior at the *N–I* phase transition. In the last few decades, the mean field model has been found to be unsuccessful in explaining the experimental observations from linear and non-linear dielectric permittivity studies. Recently, a fluid like model [34, 35] has been proposed which has successfully described the pretransitional behavior at the *N–I* transition. According to this model, the temperature dependence of the isotropic dielectric permittivity can be well described by the following fluid-like equation [29, 30, 33, 35, 36]:

$$\varepsilon_{iso}(T) = \varepsilon^* + a_T(T - T^*) + A_T(T - T^*)^{1-\alpha} \qquad (5.1)$$

where T^* represents the extrapolated temperature of a virtual continuous phase transition. ε^* is the value of ε_{iso} at $T = T^*$. a_T and A_T refer to the critical amplitudes and α is the critical exponent similar to the specific heat capacity critical exponent.

In this study, all the hockey stick-shaped compounds were heated to 15 ° to 20 °C above the sample clearing temperature (T_{NI}) and then the dielectric permittivity data were recorded upon slow cooling (rate 0.5 °C min^{-1}) at a frequency of 10 kHz. The temperature dependences of ε_{iso} for all the compounds so obtained were fitted with equation (5.1). An overview of the temperature-dependent variation of ε_{iso} for all the compounds is shown in figure 5.4. The fits to equation (5.1) are displayed as solid lines and the corresponding outcomes for the fit parameters are listed in table 5.1. As reflected from table 5.1, the extracted α values lie between 0.498 and 0.508 for the different compounds and thereby concurs well with the tricritical hypothesis (TCH) (α_{TCH} = 0.5) of Keyes [37] and Anisimov *et al.* [38, 39], indicating a first-order character of the *N–I* transition. Furthermore, the discontinuity of the *N–I* transition ΔT^*(= T_{NI} - T^*) has been found to be in the range of 5.5–9 K for the

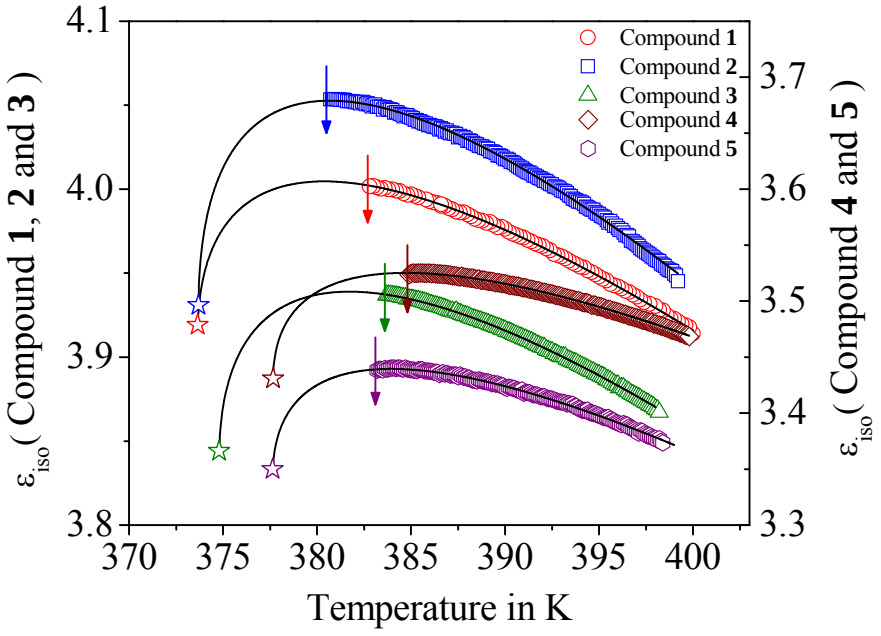

Figure 5.4. Temperature dependent variation of the dielectric permittivity (ε_{iso}) in the isotropic phase for the compounds **1**–**5**. The solid lines are fit to equation (5.1). Star symbol presents the fitted dielectric permittivity value corresponding to the temperature T^*. Arrow denotes the nematic–isotropic phase transition temperature (T_{NI}).

compounds under investigation, being least for compound **5**. This discontinuity may be treated as a measure of the bending in the temperature dependence of ε_{iso}, being less for a greater bending and vice-versa. Hence, in this study a relatively small ΔT^* value for compound **5** indicates a greater bending of ε_{iso} vs. T curve close to the N–I phase transition perhaps owing to greater pre-nematic fluctuations induced by the pseudo nematic domains formed within the isotropic phase.

Table 5.1. Results corresponding to the fit for ε_{iso} in the isotropic phase obtained in accordance with equation (5.1).

Comp-ound	T^* in K	ε^*	a_T	A_T	α
1	373.6 ± 1.6	3.91 ± 0.02	-0.0138 ± 0.0003	0.0051 ± 0.0004	0.498 ± 0.009
2	373.7 ± 0.9	3.93 ± 0.02	-0.0177 ± 0.0003	0.0087 ± 0.0004	0.502 ± 0.006
3	374.8 ± 0.7	3.84 ± 0.01	-0.0142 ± 0.0002	0.0055 ± 0.0002	0.508 ± 0.004
4	377.7 ± 0.5	3.43 ± 0.01	-0.0134 ± 0.0001	0.0050 ± 0.0003	0.501 ± 0.003
5	377.6 ± 0.6	3.34 ± 0.02	-0.0151 ± 0.0005	0.0056 ± 0.0004	0.507 ± 0.007

5.4. Elastic constant measurements

In the present system, an electrically driven Freedericksz transition was achieved in the N and Sm-C_s phases by applying a threshold field (V_{th}) of about 2–3.5 V and 3.5–4 V respectively. The voltage dependence of the capacitance for compound **3** filled planar cell (thickness 5 μm) has been presented in figure 5.5. For all the compounds, the Freedericksz threshold increases more or less monotonically with lowering of temperature and then exhibits a continuous variation across the Sm-C_s–N transition. Such a smooth change may be

attributed to the short range smectic fluctuations existing throughout the *N* phase. However, a finite discontinuity is observed in the measured value of V_{th} at the Sm-C_a–*N* or Sm-C_a–Sm-C_s transition with V_{th} attaining a value of about 10.5 V, after which the threshold again continues to increase with further lowering of temperature.

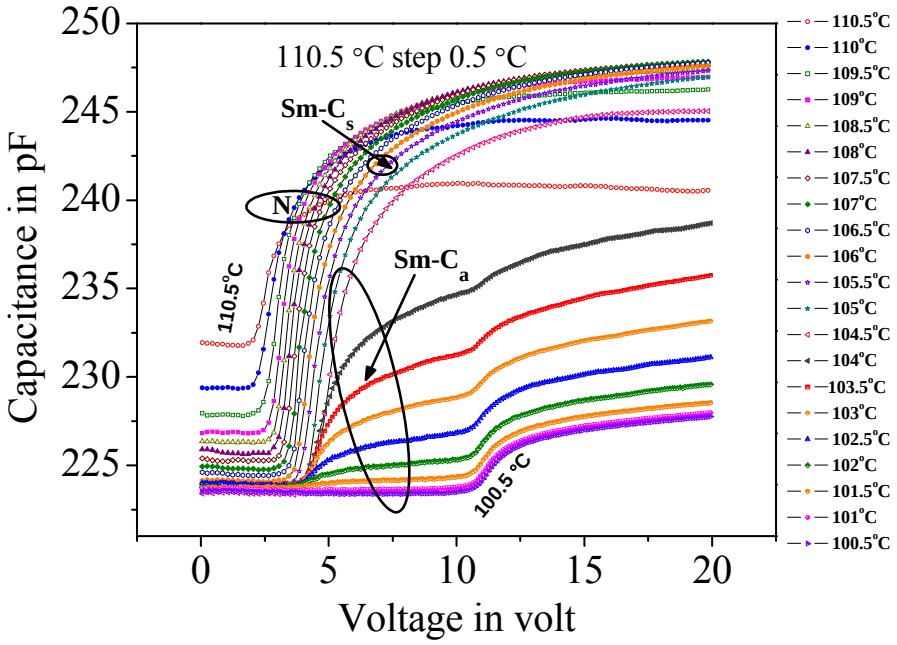

Figure 5.5. Voltage dependence of the capacitance of the sample-filled planar cell at different temperatures for compound **3**.

Figures 5.6(a)–(b) depict the temperature dependence of the splay (K_{11}) and bend (K_{33}) elastic moduli for the four hockey stick-shaped molecules **1**–**4**. In the *N* phase, it is observed that the splay modulus exhibits a linear enhancement in magnitude from ~ 0.5 pN to ~ 6–8 pN with decrease in temperature. In agreement with the continuous nature of the variation of the V_{th} values, the K_{11} values too show no pretransitional divergence in the vicinity of the nematic to the low temperature smectic phase transition. The bend elastic constant (K_{33}) however, is more or less independent of temperature in the entire nematic range except for compounds **1** and **2**, where a strong divergence is observed on approaching the low temperature anticlinic smectic phase perhaps

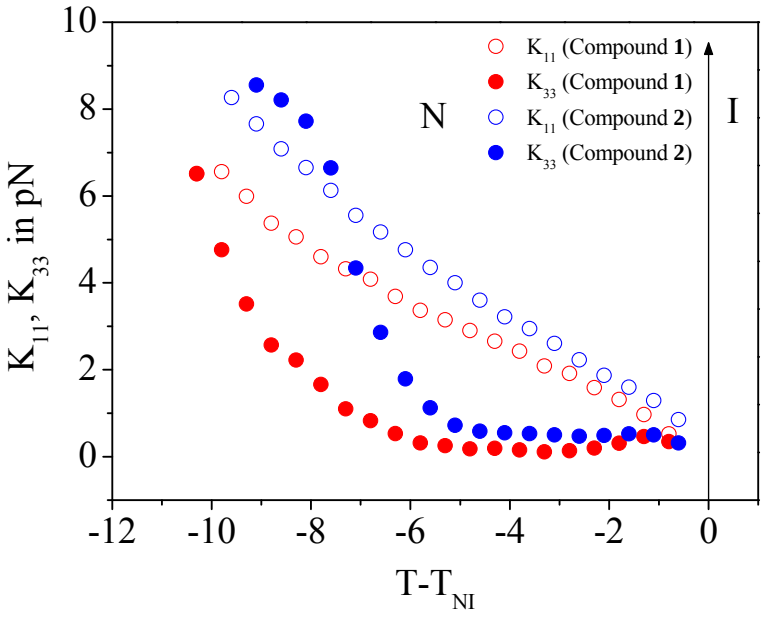

(a)

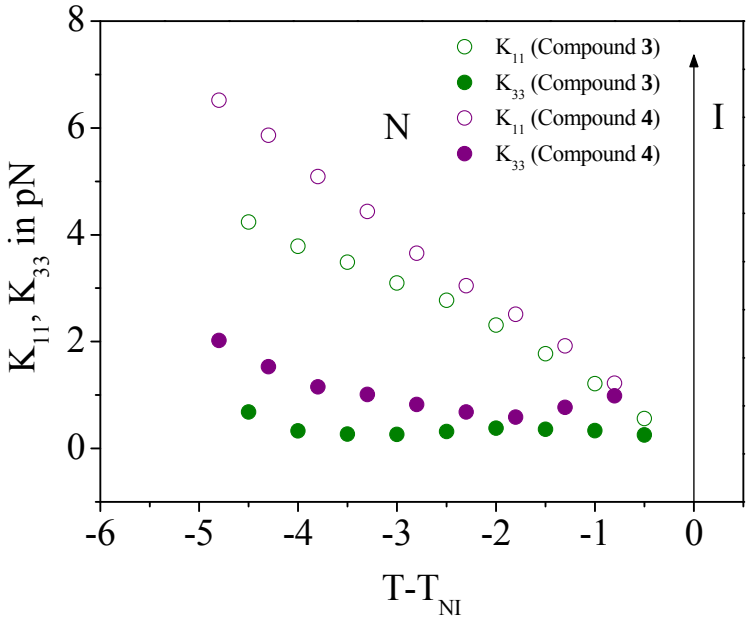

(b)

Figure 5.6. Temperature dependence of the splay (K_{11}) and bend (K_{33}) elastic constants for (a) compound **1** and compound **2**; (b) compound **3** and compound **4**.

due to the pre-smectic type influences. Such divergence in K_{33} values has also been revealed for rod-like and other various reduced symmetry molecules by different research groups [24, 40–42] as well as in converse, for a few other bent-core compounds the absence of any trace of pre-transitional divergence have also been reported [17, 43]. However, for bent-core nematogens the non-existence of any divergence for K_{11} clearly infers the contradiction to the theories developed by de Gennes [44] and Chen and Lubensky [45] predicting divergence of all the three components of Frank elastic constants near the Sm-*C*–*N* transition.

The most intriguing feature is that although the values of K_{33} near the clearing temperature and close to the Sm-C_a–*N* transition are comparable to those for K_{11}, well within the nematic phase the values of K_{33} are always substantially smaller than the corresponding K_{11} values giving rise to negative values of the elastic anisotropy (K_{33} - K_{11}) with K_{33} achieving values even less than one fourth of that of K_{11}. Such an atypical behavior is nearly non-existent in the field of conventional calamitic LCs. Nevertheless, the present result is in good agreement with the previous findings for the bent-core resorcinol derivatives (as mentioned in chapter 3) as well as with that of others for distinct bow-shaped nematogens embracing diverse form of core structures [17, 19, 24, 43, 46]. For a number of symmetric and asymmetric bent-shaped nematogens it has been found that the elastic anisotropy remains negative in the entire nematic range with K_{33} being either independent of or reluctantly dependent on temperature, while in some cases K_{33} is found to be strongly diverging on approaching the low temperature higher ordered phase. Sathyanarayana *et al.* [24] have accounted for such behavior by considering the coupling of the kink shape of the molecules with the bend-distortion in the medium leading to lower effective K_{33} values, while, Majumdar *et al.* [46] have suggested that along with the molecular shape, the formation of the highly correlated local domains with tilted smectic configuration also remarkably influences the softening of both K_{22} and K_{33} relative to K_{11}. From atomistic modeling calculations, Cestari

et al. [47, 48] have shown that a minor diversity in the extent of curvature in the bent molecular conformation has a dramatic influence on the bend elastic constant while a strong enhancement in the molecular non-linearity can deliberately reduce K_{33} and even may yield negative values for a significantly higher ordering. Recently, for an oxadiazole bent-core material Kaur *et al.* [43] have also reached the same conclusion evoking the extreme dependence of K_{33} on the structural geometry, especially on the magnitude of bend in the core moiety. They have also argued that for bent-core molecules along with the molecular form and population of conformers, the possibility of the existence of short range cybotactic clusters can merely lead to a state where the effective molecular width (W_{eff}) becomes greater than the length (L) of the molecules and thereby results in a smaller value of K_{33} than K_{11}. The present hockey stick-shaped compounds also possess a more or less bent molecular shape. Here, the steric interaction between the methyl group and the neighboring alkoxy chain in *meta*-position perhaps induces a more rod-like shape thereby facilitating the formation of the nematic phase at higher temperatures. However it is probable that the divergence from the angular shape is not very significant which perhaps leads to a considerably smaller value of K_{33}. The K_{33} values as obtained from the experimental data are of the order of 1–2 pN which are nearly of the same order for symmetric bent-core molecules. Moreover, small angle X-ray diffraction measurements also clearly indicate a smectic like short range ordering, present as an intrinsic part of the nematic phase structure, which further lowers K_{33} by enhancing the effective molecular width.

5.5. Rotational viscosity measurements

The molecular relaxation time (τ_0) was determined in the nematic phase from both the optical and capacitive study of the molecular decay dynamics. For all the four samples (compounds **1**–**4**) the temperature dependant variations of the relaxation time (τ_0) are presented in figures 5.7(a)–(b). It is observed that the results obtained from the two independent methods are in good agreement

with one another, having a small difference of about 10%–15%. Determination of rotational viscosity (γ_1) was also carried out by utilizing equation (2.19) and the temperature dependences of the same are illustrated in figures 5.8(a)–(b). Rotational viscosity is found to assume values between ~ 30 mPa s and 90 mPa s in the immediate vicinity of the *N*–*I* transition, following which it increases monotonically with decreasing temperature, certainly due to an increase in the orientational ordering of the mesogenic medium and finally diverges on approaching the low temperature smectic phase. Recently a number of experimental studies revealed that the rotational viscosity assumes dramatically high values for angular mesogenic structures [16, 17, 19], in some circumstances being nearly an order of magnitude higher than those of normal calamitics. Such an intriguing behavior has been attributed to the formation of smectic-like clusters utilizing the shape anisotropy and the strong transverse dipolar contribution, emerging from the kink shape of the bent-core molecules [16]. The occurrence of such clusters and their rigorous influence on the phase behavior of bent-core nematics has also been demonstrated by different research groups [12, 46, 49–53]. As stated above, for the system under study, small angle X-ray data also clearly validates the presence of such short range Sm-*C* like ordering. However, despite such clustering, the γ_1 values are found to be considerably smaller than in many pure bent-core systems [16, 17]. Moreover, these values are slightly higher than those obtained for several usual calamitic systems and their mixtures [14, 15]. In spite of the presence of bend, such a calamitic like behavior is perhaps due to the fact that the steric interaction between the methyl group and the neighboring alkoxy chain in meta position of the terminal phenyl ring possibly partially trims down the effect of molecular curvature, thereby lowering the short range macroscopic clustering effect to some extent over the mesomorphic range.

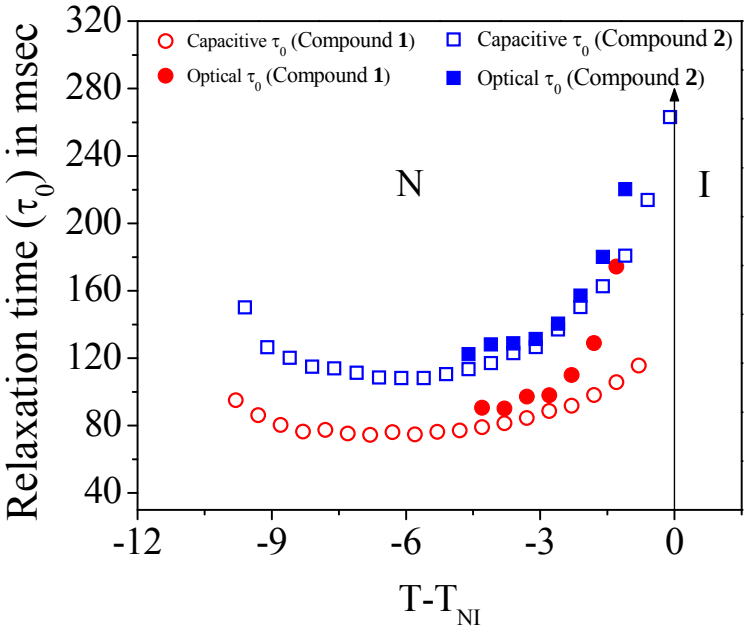

(a)

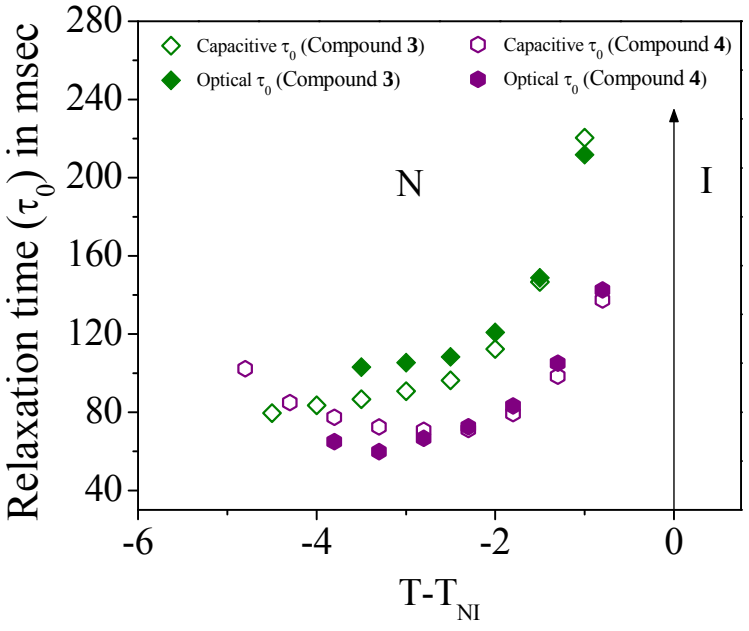

(b)

Figure 5.7. Temperature dependence of the relaxation time (τ_0) in the nematic phase for (a) compound **1** and compound **2**; (b) compound **3** and compound **4** measured from both optical method and capacitance method.

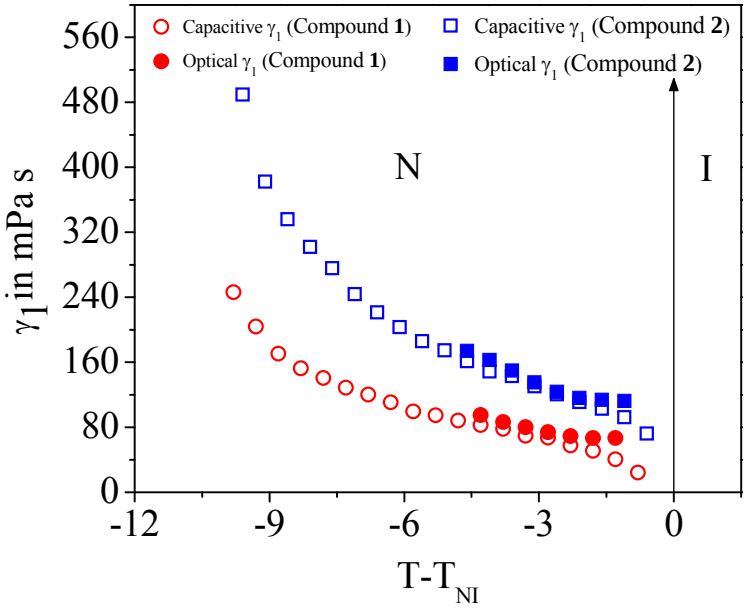

(a)

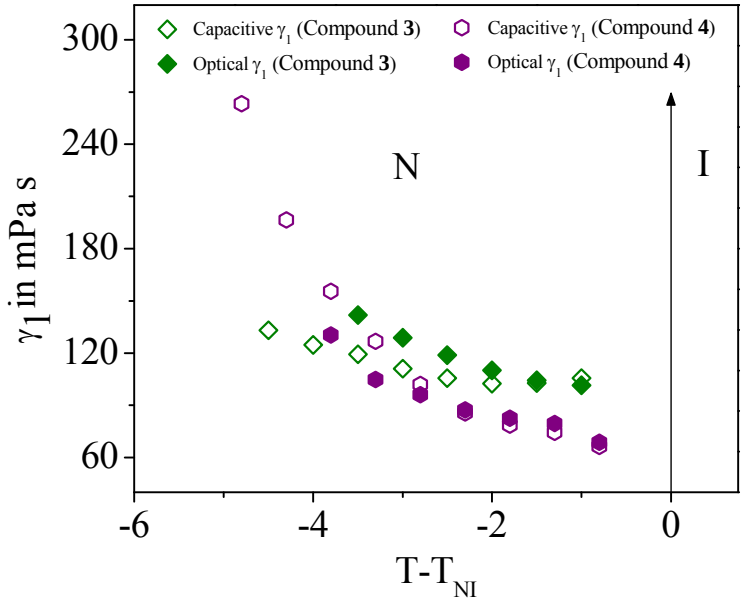

(b)

Figure 5.8. Temperature dependence of the rotational viscosity (γ_1) in the nematic phase for (a) compound **1** and compound **2**; (b) compound **3** and compound **4** as obtained from both optical and capacitance method.

The temperature dependence of γ_1 was fitted with equation (3.5) using the values of the orientational order parameter (S) determined from birefringence measurement. The variations of $\ln(\gamma_1/S)$ with $1/T$ for compound **1** from capacitance measurement is illustrated in figure 5.9. From the slope of the curve the associated activation energy (E_a) can be evaluated. Activation energy is found to be about 145 kJ mol^{-1} and 153 kJ mol^{-1} for compounds **1** and **2** respectively. However, due to the limited range of the nematic phase, it was not possible to measure the E_a values with the desired degree of accuracy for compounds **3** and **4** because of the unavailability of an adequate number of data points. It is observed that the measured E_a values are about an order of magnitude higher than those for conventional calamitic molecules. Probably in the vicinity of phase transitions, due to the rapid increase in the cluster size, the molecular motion is affected by the strong pretransitional fluctuations leading to such quite high E_a values. However, as the E_a values obtained are the

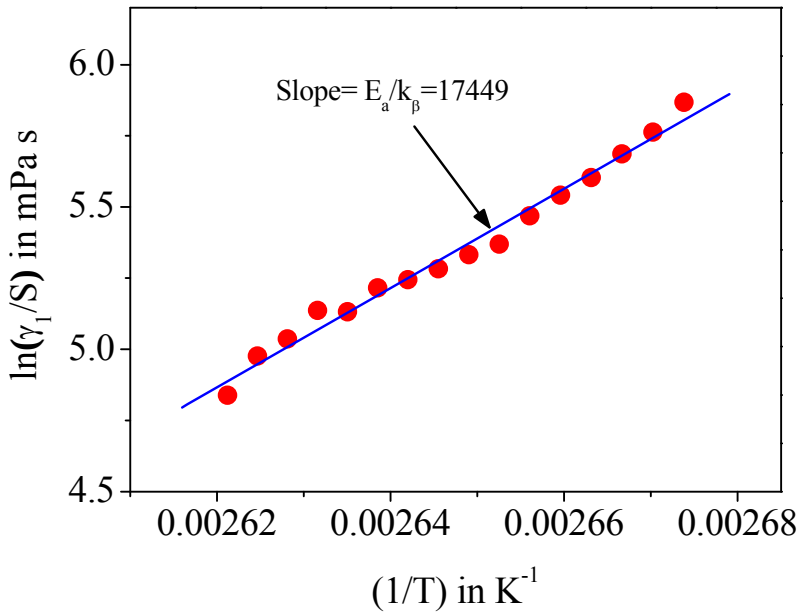

Figure 5.9. Variation of $\ln(\gamma_1/S)$ with $(1/T)$ for compound **1** (●) from capacitance method. Solid line (—) represents best fit of the data to equation (3.5).

average over the entire *N* phase, the narrowness of the *N* phase and the presence of strong correlation among the smectic like structural aggregates may also be responsible for such high activation energies. The occurrence of high activation energy near the transition concurs well with the findings of Jadżyn *et al.* [32] from dielectric measurements in rod-like molecules.

The molecular curvature and inter-molecular interactions certainly have a remarkable influence on the phase behavior and structure-property correlations of bent-shaped nematogens. Unlike interactions in conventional nematics, comprising only nearest neighbor correlations, the shape induced periodic interactions suffered by the bent molecules preferably lead to a simultaneous breaking of translational symmetry along the molecular long axis facilitating the formation of short range structural aggregates of the smectic type, persisting as an intrinsic part of the nematic phase structure throughout the mesophase. Furthermore, it has also been observed that for bent molecules a small modification in the molecular conformation and bend can significantly alter the phase behavior of the concerned mesogen [54]. Hockey stick-shaped mesogens have a molecular shape neither rod-like nor banana-shaped with the location of the bend quite shifted from the centre of the molecular core therefore exhibiting a number of mesophase sequences and phase characteristics intermediate between that for the classical calamitic and banana shaped molecules [55, 56]. For instance, despite the shape non-linearity for a group of five ring hockey stick-shaped materials with ester linkage, Novotná and others have observed no trace of dipolar order in the tilted smectic phases [57] perhaps indicating the absence of banana like packing, i.e., revealing a more rod-like behavior. Furthermore, as described in the previous chapter (chapter 4) conductivity measurements on the present hockey stick molecules also did not yield a conclusive polar answer.

Hence, in this study a fascinating alliance of both rod-like properties (as to the magnitude and temperature variation of γ_1) and angular like behavior (as to the temperature variation of dielectric constants and elastic moduli) has been

explored for the similar molecules. Such a remarkable feature is perhaps due to the collective domination of both the molecular curvature and segregation, on the static and dynamic behavior of bent molecules; however, the dependency on these two factors gets varied from one property to another one. Recently, for a five-ring achiral hockey stick-shaped nematogen the γ_1 values have been found to be considerably higher than for classical calamitic ones [19]. Such a behavior is explained as partially due to the greater molecular weight of hockey stick molecules and to the presence of cybotactic clusters emerging from the rotational hindrance along the long axis of bent molecules. Comparing the present hockey stick-shaped compounds (3 aromatic rings) with those reported in Ref. [19] (5 aromatic rings) and with conventional bent-core compounds (in general 5 aromatic rings or more) their smaller aromatic cores and alkyl chains certainly induce less clustering in the nematic range.

5.6. Conclusions

A systematic physical investigation has been carried out in the nematic phase of a few hockey stick-shaped liquid crystals with a laterally attached methyl group in the molecular core between the *m*-alkyloxy chain and azomethine connection group from optical birefringence, static dielectric, splay and bend elastic constants, relaxation time and rotational viscosity measurements. From birefringence measurements it has been observed that the Sm-C_a–*N* transition is of first order while the Sm-C_s–*N* transition is either of second order or weakly first order. The temperature variation of the dielectric permittivity exhibits a strong dependence on the anisotropic correlations among the hockey stick-shaped molecules while the dielectric anisotropy undergoes a sign-reversal from positive to negative values on entering the Sm-C_a phase, conceivably due to a substantial enhancement in the antiparallel dipolar correlation for the longitudinal dipolar component. From an analysis of the temperature dependence of dielectric permittivity in the isotropic phase, the pretransitional behavior at the nematic–isotropic phase transition has also been

explored. The extracted critical exponent (α) values have been found to be close to 0.5 and thus are in agreement with the tricritical hypothesis. Similar to the traditional bent-core compounds, in the present system as well, the bend elastic modulus (K_{33}) was found to be significantly smaller than the splay one (K_{11}), perhaps owing to the collective influence of both the coupling between the curved molecular profile and the bend deformation in the medium as well as the existence of comparatively highly ordered molecular aggregates within the *N* phase. Furthermore, although existing theoretical models demand the occurrence of a pretransitional divergence in the vicinity of the Sm-*C* phase for all the components of the curvature elastic constant (K_{ii}), in the present study the K_{11} data do not demonstrate any such behavior, indicating an insufficiency of those models for dealing with bent-core as well as with hockey stick-shaped nematogens. Surprisingly, the measured nematic rotational viscosity (γ_1) values being in the order of few tens to few hundreds of mPa s, certainly characterize the present materials with a more or less calamitic like behavior and thereby contradict the banana like appearance asserted by the elastic constant measurements. Such a fascinating outcome can merely be accounted for by considering the fact that like in conventional bent core compounds, for hockey stick-shaped nematogens as well, different shape correlated molecular interactions and eccentric phase-structure modifications (e.g., strong rotational hindrance, significant clustering within the mesophase) take place but to a somewhat less extent and that is why they promote a number of such remarkable phenomena some of which pertain to calamitic LCs while some other are related to the bent core compounds, again some are completely intermediate between both of them. However, the entire scenario is still not clear requiring further investigations including synthesis of new mesogenic compounds with a variety of conformations and also detailed theoretical approaches.

References:

[1] J. Harden, B. Mbanga, N. Éber, K. Fodor-Csorba, S. Sprunt, J. T. Gleeson, and A. Jákli, *Phys. Rev. Lett.*, **97**, 157802 (2006).

[2] J. Harden, R. Teeling, J. T. Gleeson, S. Sprunt, and A. Jákli, *Phys. Rev. E*, **78**, 031702 (2008).

[3] D. Wiant, J. T. Gleeson, N. Éber, K. Fodor-Csorba, A. Jákli, and T. Tóth-Katona, *Phys. Rev. E*, **72**, 041712 (2005).

[4] S. Tanaka, S. Dhara, B. K. Sadashiva, Y. Shimbo, Y. Takanishi, F. Araoka, K. Ishikawa, and H. Takezoe, *Phys. Rev. E*, **77**, 041708 (2008).

[5] S. Tanaka, H. Takezoe, N. Éber, K. Fodor-Csorba, A. Vajda, and A. Buka, *Phys. Rev. E*, **80**, 021702 (2009).

[6] P. Salamon, N. Éber, A. Buka, J. T. Gleeson, S. Sprunt, and A. Jákli, *Phys. Rev. E*, **81**, 031711 (2010).

[7] T. Ostapenko, D. B. Wiant, S. N. Sprunt, A. Jákli, and J. T. Gleeson, *Phys. Rev. Lett.*, **101**, 247801 (2008).

[8] B. R. Acharya, A. Primak, T. J. Dingemans, E. T. Samulski, and S. Kumar, *Pramana*, **61**, 231 (2003).

[9] L. A. Madsen, T. J. Dingemans, M. Nakata, and E. T. Samulski, *Phys. Rev. Lett.*, **92**, 145505 (2004).

[10] B. R. Acharya, A. Primak, and S. Kumar, *Phys. Rev. Lett.*, **92**, 145506 (2004).

[11] R. Stannarius, A. Eremin, M. –G. Tamba, G. Pelzl, and W. Weissflog, *Phys. Rev. E*, **76**, 061704 (2007).

[12] O. Francescangeli, V. Stanic, S. I. Torgova, A. Strigazzi, N. Scaramuzza, C. Ferrero, I. P. Dolbnya, T. M. Weiss, R. Berardi, L. Muccioli, S. Orlandi, and C. Zannoni, *Adv. Funct. Mater.*, **19**, 2592 (2009).

[13] S. T. Wu, *J. Appl. Phys.*, **60**, 1836 (1986).

[14] S. T. Wu and C. S. Wu, *Phys. Rev. A*, **42**, 2219 (1990).

[15] M. L. Dark, M. H. Moore, D. K. Shenoy, and R. Shashidhar, *Liq. Cryst.*, **33**, 67 (2006).

[16] E. Dorjgotov, K. Fodor-Csorba, J. T. Gleeson, S. Sprunt, and A. Jákli, *Liq. Cryst.*, **35**, 149 (2008).

[17] P. Tadapatri, U. S. Hiremath, C. V. Yelamaggad, and K. S. Krishnamurthy, *J. Phys. Chem. B*, **114**, 1745 (2010).

[18] P. Sathyanarayana, T. A. Kumar, V. S. S. Sastry, M. Mathews, Q. Li, H. Takezoe, and S. Dhara, *Appl. Phys. Express*, **3**, 091702 (2010).

[19] P. Sathyanarayana, S. Radhika, B. K. Sadashiva, and S. Dhara, *Soft Matter*, **8**, 2322 (2012).

[20] A. Chakraborty, M. K. Das, B. Das, U. Baumeister, and W. Weissflog, *J. Mater. Chem. C*, **1**, 7418 (2013).

[21] A. Prasad and M. K. Das, *J. Phys.: Condens. Matter*, **22**, 195106 (2010).

[22] J. A. Olivares, S. Stojadinovic, T. Dingemans, S. Sprunt, and A. Jákli, *Phys. Rev. E*, **68**, 041704 (2003).

[23] G. Sarkar, B. Das, M. K. Das, U. Baumeister, and W. Weissflog, *Mol. Cryst. Liq. Cryst*., **540**, 188 (2011).

[24] P. Sathyanarayana, M. Mathew, Q. Li, V. S. S. Sastry, B. Kundu, K. V. Le, H. Takezoe, and S. Dhara, *Phys. Rev. E*, **81**, 010702 (2010).

[25] W. H. de Jeu, T. W. Lathouwers, and P. Bordewijk, *Phys. Rev. Lett.*, **32**, 40 (1974).

[26] B. Das, S. Grande, W. Weissflog, A. Eremin, M. W. Schröder, G. Pelzl, S. Diele, and H. Kresse, *Liq. Cryst*., **30**, 529 (2003).

[27] W. Maier and G. Meier, *Z. Naturforsch A*, **16a**, 262 (1961).

[28] S. Chandrasekhar, *Liquid Crystals*, Cambridge University Press, Cambridge (1992).

[29] A. Drozd-Rzoska, S. J. Rzoska, and J. Ziolo, *Phys. Rev. E*, **54**, 6452 (1996).

[30] S. J. Rzoska, J. Ziolo, W. Sulkoski, J. Jadżyn, and G. Czechowski, *Phys. Rev. E*, **64**, 052701 (2001).

[31] M. Ginovska, H. Kresse, D. Bauman, G. Czechowski, and J. Jadzyn, *Phys. Rev. E*, **69**, 022701 (2004).

[32] J. Jadżyn, G. Czechowski and J. -L. Déjardin, *J. Phys.: Condens. Matter*, **18**, 1839 (2006).

[33] S. K. Sarkar and M. K. Das, *Fluid Phase Equilibria*, **365**, 41 (2014).

[34] P. K. Mukherjee and T. B. Mukherjee, *Phys. Rev. B*, **52**, 9964 (1995).

[35] P. K. Mukherjee, *J. Phys.: Condens. Matter*, **10**, 9191 (1998).

[36] A. Drozd-Rzoska, *Phys. Rev. E*, **59**, 5556 (1999).

[37] P. H. Keyes, *Phys. Lett. A*, **67**, 132 (1978).

[38] M. A. Anisimov, S. R. Garber, V. S. Esipov, V. M. Mamnitskii, G. I. Ovodov, L. A. Smolenko, and E. L. Sorkin, *Sov. Phys. JETP*, **45**, 1042 (1977).

[39] M. A. Anisimov, *Mol. Cryst. Liq. Cryst. Inc. Nonlinear Opt.*, **162**, 1 (1988).

[40] S. W. Morris, P. Palffy-Muhoray, and D. A. Balzarini, *Mol. Cryst. Liq. Cryst.*, **139**, 263 (1986).

[41] M. R. Dodge, R. G. Petschek, C. Rosenblatt, M. E. Neubert, and M. E. Walsh, *Phys. Rev. E*, **68,** 031703 (2003).

[42] P. Sathyanarayana, M. C. Varia, A. K. Prajapati, B. Kundu, V. S. S. Sastry, and S. Dhara, *Phys. Rev. E*, **82**, 050701 (2010).

[43] S. Kaur, J. Addis, C. Greco, A. Ferrarini, V. Görtz, J. W. Goodby, and H. F. Gleeson, *Phys. Rev. E*, **86**, 041703 (2012).

[44] P. G. de Gennes, *Mol. Cryst. Liq. Cryst.*, **21**, 49 (1973).

[45] J. -H. Chen and T. C. Lubensky, *Phys. Rev. A*, **14**, 1202 (1976).

[46] M. Majumdar, P. Salamon, A. Jákli, J. T. Gleeson, and S. Sprunt, *Phys. Rev. E*, **83**, 031701 (2011).

[47] M. Cestari and A. Ferrarini, *Soft Matter*, **5**, 3879 (2009).

[48] M. Cestari, E. Frezza, A. Ferrarini, and G. R. Luckhurst, *J. Mater. Chem.*, **21**, 12303 (2011).

[49] S. Stojadinovic, A. Adorjan, S. Sprunt, H. Sawade, and A. Jákli, *Phys. Rev. E*, **66**, 060701 (2002).

[50] N. Vaupotič, J. Szydlowska, M. Salamonczyk, A. Kovarova, J. Svoboda, M. Osipov, D. Pociecha, and E. Gorecka, *Phys. Rev. E*, **80**, 030701 (2009).

[51] C. Bailey, K. Fodor-Csorba, J. T. Gleeson, S. N. Sprunt, and A. Jákli, *Soft Matter*, **5**, 3618 (2009).

[52] C. Keith, A. Lehmann, U. Baumeister, M. Prehm, and C. Tschierske, *Soft Matter*, **6**, 1704 (2010).

[53] O. Francescangeli and E. T. Samulski, *Soft Matter*, **6**, 2413 (2010).

[54] K. M. Fergusson and M. Hird, *J. Mater. Chem*., **20**, 3069 (2010).

[55] F. C. Yu and L. J. Yu, *Chem. Mater*., **18**, 5410 (2006).

[56] F. C. Yu and L. J. Yu, *Liq. Cryst*., **35**, 799 (2008).

[57] V. Novotná, J. Žurek, V. Kozmík, J. Svoboda, M. Glogarová, J. Kroupa, and D. Pociecha, *Liq. Cryst*., **35**, 1023 (2008).